



Allosteric inhibition of HIF-2 as a novel therapy for clear cell renal cell carcinoma

Yancheng Yu, Quanwei Yu and Xiaojin Zhang

Jiangsu Key Laboratory of Drug Design and Optimization, and Department of Chemistry, China Pharmaceutical University, Nanjing 211198, China



Clear cell renal cell carcinoma (ccRCC) is the most common subtype of RCC and bears a significantly high frequency of hypoxia-inducible factor 2 α (HIF-2 α) because of von Hippel-Lindau (*VHL*) tumor suppressor gene mutations. From the first discovery of HIF-2 α inhibitors to the promising potency of the HIF-2 α inhibitor PT2977 in a clinical Phase II trial for the treatment of advanced RCC, inhibition of HIF-2 α has proved to be a novel and effective therapy for RCC. In this review, we briefly discuss the role of HIF-2 α in ccRCC and provide insight into recent advances in the discovery, development, and mode of action of HIF-2 α allosteric inhibitors.

Introduction

RCC or kidney cancer is the second leading cause of urinary cancer death worldwide. Metastasis and chemotherapy resistance are characteristics of RCC [1]. ccRCC, the most common subtype, accounts for 85% of RCC. Integrated molecular studies of ccRCC indicated that inactivation of the *VHL* gene was a common feature of ccRCC (90%) [2]. The VHL protein acts as a substrate recognition component of an E3 ubiquitin ligase complex that targets HIF-1 α and HIF-2 α for degradation via the ubiquitin-proteasome pathway [3,4]. Loss of VHL leads to the accumulation of HIF- α and subsequent uncontrollable activation of HIF target genes, many of which facilitate angiogenesis, proliferation, and metastasis of ccRCC [5]. HIF-1 and HIF-2 are the two most important subtypes of HIFs, comprising a HIF α subunit and aryl hydrocarbon receptor nuclear translocator (ARNT) subunit. Many studies suggest that HIF-1 and HIF-2 display distinct effects in ccRCC: HIF-2 is a key oncoprotein; however, the role of HIF-1 appears to be as a tumor suppressor [6,7]. Previously, HIF-2 was considered a challenging target for drug design because it did not have any catalytic sites for small-molecule binding. In 2009, Gardner *et al.* revealed a cavity inside HIF-2 α and some leads that could bind with the cavity to alter its conformation and thereby disturb the activity of the HIF-2 complex [8,9]. Therefore, inhibition of HIF-2 α has become a new strategy for the treatment of RCC. Currently, the HIF-2 α inhibitor

PT2977 of Peloton Therapeutics, Inc. is undergoing clinical Phase II trials for advanced RCC and shows favorable safety profile and efficacy [10]. In this review, we discuss the allosteric inhibition mechanism and outline recent advances in the development in HIF-2 α allosteric inhibitors.

Regulation of HIF-2

HIF-2 is a heterodimeric transcription factor complex comprising the oxygen-sensitive HIF-2 α subunit and the constitutively expressed partner ARNT subunit. The two subunits belong to the basic helix-loop-helix (bHLH)-Per-ARNT-Sim (PAS) family and contain a similar bHLH domain (DNA-binding domain, DBD) and PAS domain (ligand-binding domain, LBD). The PAS domain comprises two domains, PASA and PASB. In addition, HIF-2 α comprises two relatively independent transactivation domains, the N-terminal transactivation domain (NTAD) and C-terminal transactivation domain (CTAD), and the oxygen-dependent degradation domain (ODD) [11] (Fig. 1a).

Under normoxic conditions, Pro405 and Pro531 in the ODD can be hydroxylated by proline hydroxylases (PHDs) with the participation of oxygen, iron ions, and α -ketoglutarate. Subsequently, hydroxylated HIF-2 α is ubiquitinated by the E3 ligase complex for proteasome degradation [4]. Meanwhile, the Asn847 in the CTAD can be hydroxylated by factor inhibiting HIF (FIH), and this leads to inhibition of the transactivation function of CTAD [12,13] (Fig. 1c). Under low oxygen conditions, the hydroxylation ability

Corresponding author: Zhang, X. (zxj@cpu.edu.cn)

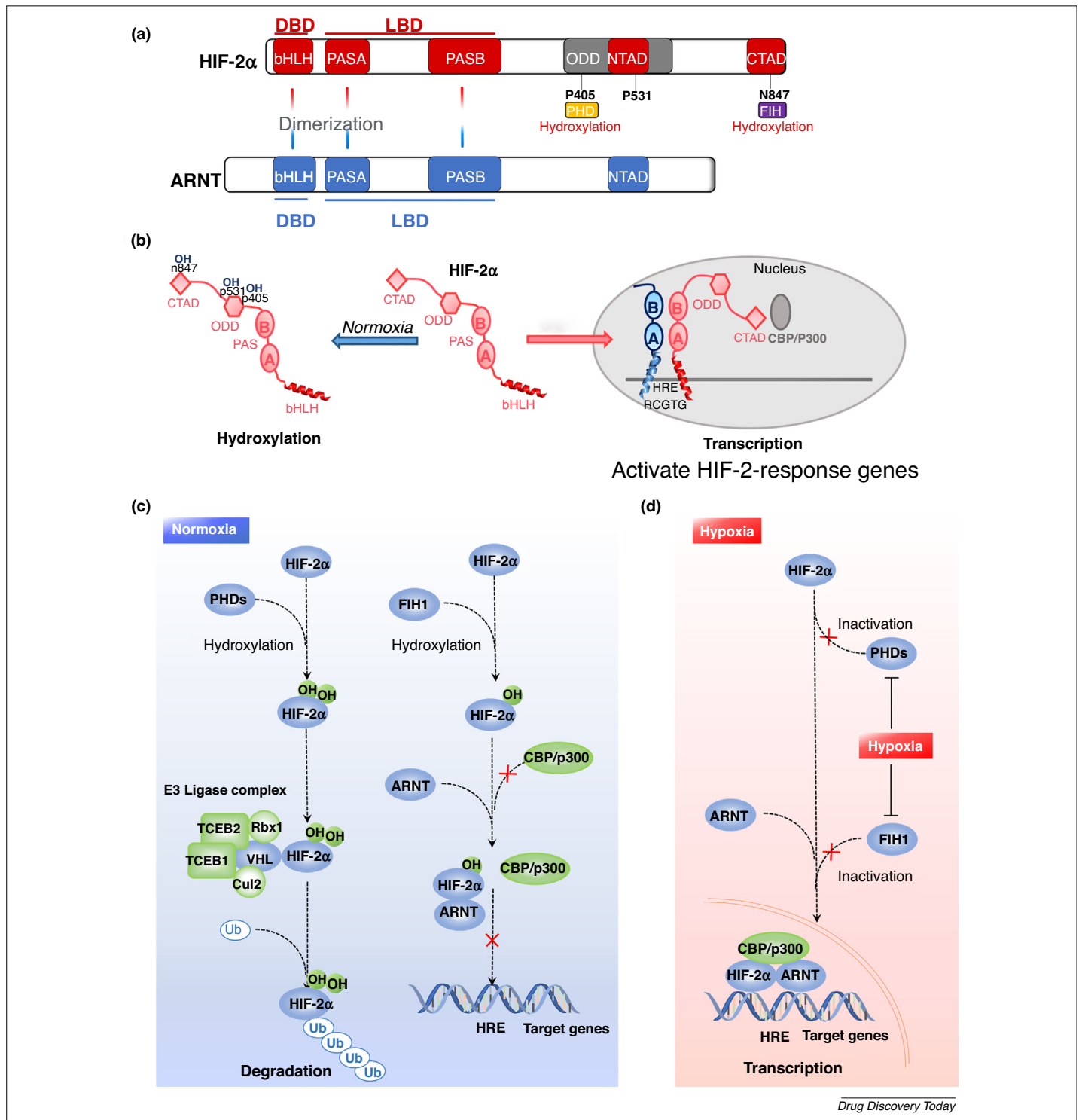


FIGURE 1

Overview of the structures, features, and regulation of hypoxia-inducible factor 2 (HIF-2). **(a)** Schematic representation showing the domain arrangements of aryl hydrocarbon receptor nuclear translocator (ARNT; blue) and HIF-2 α (red). **(b)** HIF regulation is tightly linked to intracellular oxygen levels. Under normoxic conditions; HIF-2 α is hydroxylated by proline hydroxylases (PHDs) and factor inhibiting HIF (FIH); modification of Pro405 and Pro531 in the oxygen-dependent degradation domain (ODD) promote the degradation of HIF-2 α ; modification of Asn847 in the C-terminal transactivation domain (CTAD) interferes with its ability to interact with CBP/P300 coactivators. These modifications are inhibited under hypoxic conditions: HIF-2 α (red) accumulates and translocates to the nucleus, where it associates with ARNT (blue) and binds to hypoxia response elements (HREs) to activate HIF-2-related genes. **(c)** Under normoxic condition, HIF-2 α is hydroxylated by PHDs and then ubiquitinated by the E3 ligase complex for degradation. Additionally, hydroxylation of HIF-2 α by FIH prevents P300 and CBP from binding to CTAD and inhibits transcription. **(d)** Under hypoxic conditions, PHDs and FIH are inactivated, HIF-2 α and ARNT dimerize, enter the nucleus, and bind to HRE to activate downstream target genes. For additional abbreviations, please see the main text.

of PHDs and FIH is significantly decreased; consequently, the degradation of HIF-2 α is hindered, which allows HIF-2 α and ARNT to form a HIF-2 dimer that enters into the nucleus. Subsequently, the bHLH domain of HIF-2 binds to the hypoxia response element (HRE) and the CTAD recruits the coregulators CBP/P300, leading to co-activation of HIF-2 target genes [14] (Fig. 1d).

The role of HIF-2a in ccRCC

In ccRCC, *VHL* deficiency results in the stable existence of HIF- α irrespective of oxygen tension [3]. HIF-1 α is a tumor suppressor that can inhibit the proliferation of *VHL*-deficient ccRCC both *in vitro* and *in vivo*; however, HIF-1 α expression is lost in 30–40% of cases of ccRCC. In contrast to the role of HIF-1 α , HIF-2 α acts as a key oncogenic protein in ccRCC [6,7]. The promotion of ccRCC by excessive HIF-2 α is mainly achieved by the overexpression of its target genes [5]. Therefore, the effects of HIF-2 α on ccRCC are multifaceted. Table 1 provides a summary of the HIF-2 α -related genes reported to be involved in ccRCC progression.

In ccRCC, accumulated HIF-2 α causes overexpression of many angiogenic factors, such as VEGFA [15] and its most important receptor VEGFR2 [16] encoded by *FLK1*. The binding of VEGFA–VEGFR2 is the master promoter of angiogenic effects [15]. The effect of HIF-2 α on angiogenesis is not limited to the VEGF pathway. PDGFB [17] and the ANGPT1/Tie2 [18] axis are also positively regulated by HIF-2 α to induce angiogenesis. In addition, the cytokine interleukin-6 [19], which can promote tumor angiogenesis by inducing VEGF synthesis, and adrenomedullin [20], which can protect cells from apoptosis and vascular injury, are also regulated by HIF-2 α .

Excessive HIF-2 α has also been proven to provoke tumor proliferation and survival. HIF-2 α stimulates the TGF α /EGFR pathway [21,22] to promote tumor proliferation. HIF-2 α also restrains p53 activation by upregulating antioxidant genes to reduce reactive oxygen species (ROS) levels and consequent DNA damage to facilitate tumor survival [23]. Moreover, HIF-2 α can enhance the transcriptional activity of *c-Myc* and promotes overexpression of *c-Myc* downstream genes to accelerate cell cycle progression [24,25].

Another G1/S cell cycle regulatory protein, cyclin D1, is encoded by *CCND1*. HIF-2 α can bind to the enhancer of *CCND1* to increase the expression of Cyclin D1. Studies showed that silencing *CCND1* in 786-O cell lines did not inhibit cell proliferation *in vitro*, but could significantly inhibit the formation of xenograft tumors [26]. Additionally, HIF-2 α upregulates expression of the amino acid carrier SLC7A5 to potential the activity of mTORC1, which has a crucial role in tumor cell growth and proliferation [27–29].

Furthermore, excessive HIF-2 α can also enhance the invasion and metastasis of ccRCC via the CXCR4/SDF1 α axis, which induces epithelial matrix transformation and promotes the generation of RCC-derived cancer stem cells [30,31]. Additionally, HIF-2 α promotes GAS6/AXL signaling to control the proto-oncogene *Met*; accelerating invasion and metastasis [32] and upregulating expression of matrix metalloproteases (MMPs) [33–36], CDCP1 [37], and SK1 [38] to also promote ccRCC metastasis in different ways. The metabolic process of ccRCC is also closely related to HIF-2 α . HIF-2 α accelerates cell glycolytic process by upregulating GLUT1 to adapt cells to hypoxia. In 2011, Chan *et al.* discovered that silencing *GLUT1* can promote apoptosis of the RCC cell line RCC4 [39,40]. *PLIN2*, another HIF-2 α target gene, facilitates the formation of lipid droplets in cells, which results in a clear appearance of ccRCC cells. Furthermore, lipid droplets have also been shown to have important relationships with cell survival in ccRCC [41].

In summary, uncontrolled HIF-2 α regulates the expression of hundreds of hypoxia-associated genes, some of which can promote the progress of ccRCC via various mechanisms. Compared with the current antiangiogenic therapy for the treatment of RCC, therapies targeting HIF-2 α have the potential to regulate most of the hypoxia-related signaling pathways and, thus, could be a more effective option.

HIF-2 α /ARNT allosteric inhibitors

Discovery and validation of target

Although the importance of HIF-2 α as an oncogenic protein in *VHL*-deficient ccRCC has long been widely accepted, there were few studies that explored HIF-2 α inhibitors. In 2009, Gardner *et al.*

TABLE 1
ccRCC development-related genes regulated by HIF-2

Function	Gene	Description	Refs
Angiogenesis	<i>VEGFA</i>	Vascular endothelial growth factor A	[15]
	<i>PDGFB</i>	Platelet-derived growth factor-B	[18]
	<i>FLK1</i>	Vascular endothelial growth factor receptor-2	[16]
	<i>IL-6</i>	Interleukin 6	[19]
	<i>ANGPT1/ Tie2</i>	Angiopietin proteins 1/ TEK receptor tyrosine kinase	[17]
	<i>ADM</i>	Adrenomedullin	[20]
Cell cycle and proliferation	<i>CCND1</i>	Cyclin D1	[26]
	<i>TGFα</i>	Transforming growth factor α	[21,22]
	<i>c-Myc</i>	MYC proto-oncogene	[24,25]
	<i>SLC7A5</i>	Large neutral amino acid transporter (LAT)1	[27–29]
Metastasis	<i>CXCR4</i>	C-X-C motif chemokine receptor 4	[30,31]
	<i>MMP2</i>	Matrix metalloproteinase 2	[33]
	<i>MMP9</i>	Matrix metalloproteinase 9	[34]
	<i>SK1</i>	Sphingosine kinase-1	[38]
	<i>CDCP1</i>	CUB domain-containing protein 1	[37]
	<i>GAS6/AXL</i>	Growth arrest specific 6 /AXL receptor tyrosine kinase	[32]
Metabolism	<i>SLC2A1</i>	Glucose transporter 1	[39,40]
	<i>PLIN2</i>	Perilipin 2	[41]

unexpectedly discovered that the HIF-2 α -PASB domain has a closed 290 Å³ internal cavity, which is occupied by eight ordered, bound water molecules to form a hydrogen-bonding network with polar residues [Protein Data Bank (PDB) ID: 3F1P] [8,9] (Fig. 2a). Subsequently, they obtained several lead compounds, capable of binding to this cavity, through a nuclear magnetic resonance (NMR)-based ligand screening method. Several rounds of structure–activity relationship (SAR) studies were carried out on the lead compounds to obtain a class of bicyclic molecules with high HIF-2 α -PASB domain binding affinity. **THS-044 (1)**, a compound with $K_D = 2 \mu\text{M}$ tested by isothermal titration calorimetry (ITC), was selected for follow-up studies. The crystal structure (PDB ID: 3F1O) indicated that **THS-044** occupies the cavity inside HIF-2 α -PASB and interacts with residues including His248, Tyr281, Ser292, and His293 (Fig. 2b). A ¹⁵N/¹H heteronuclear singular quantum correlation (HSQC)-based titration assay was conducted to assess the inhibitory effect of **THS-044** on the dimerization of HIF-2 α -PASB and ARNT-PASB. This assay revealed that 100 μM **THS-044** was able to significantly attenuate the stability of the PASB heterodimer, weakening its dissociation constant from

120 μM to 400 μM [8]. This demonstrated that it is feasible to perturb HIF-2 activity by binding small molecules to the cavity in the HIF-2 α -PASB domain. These bicyclic compounds are the leads for HIF-2 α inhibitors.

Structural basis of HIF-2 α allosteric inhibition

Although bicyclic compounds, such as **THS-044**, are capable of inhibiting the dimerization of HIF-2 α and ARNT, analysis of the inhibition mechanism has been limited to the HIF-2 α -PASB domain and is not clear. In 2013, Tambar *et al.* proposed a hypothesis that the internal cavity of the HIF-2 α -PASB domain can be bound by small molecules, leading to conformational changes and interruption of HIF dimerization [42]. In 2015, a crystal structure characterization that was integral to increasing understanding of HIF was reported by Wu *et al.*, analyzing all cavities of HIF that might enable small-molecule binding [11]. Then, in 2016, Josey *et al.* proposed a possible allosteric inhibition mechanism. The binding of antagonists to the HIF-2 α -PASB cavity changes the conformation of Met252, Tyr278, and His293, disturbing the dimerization of the HIF-2 α -PASB domain and ARNT-PASB domain

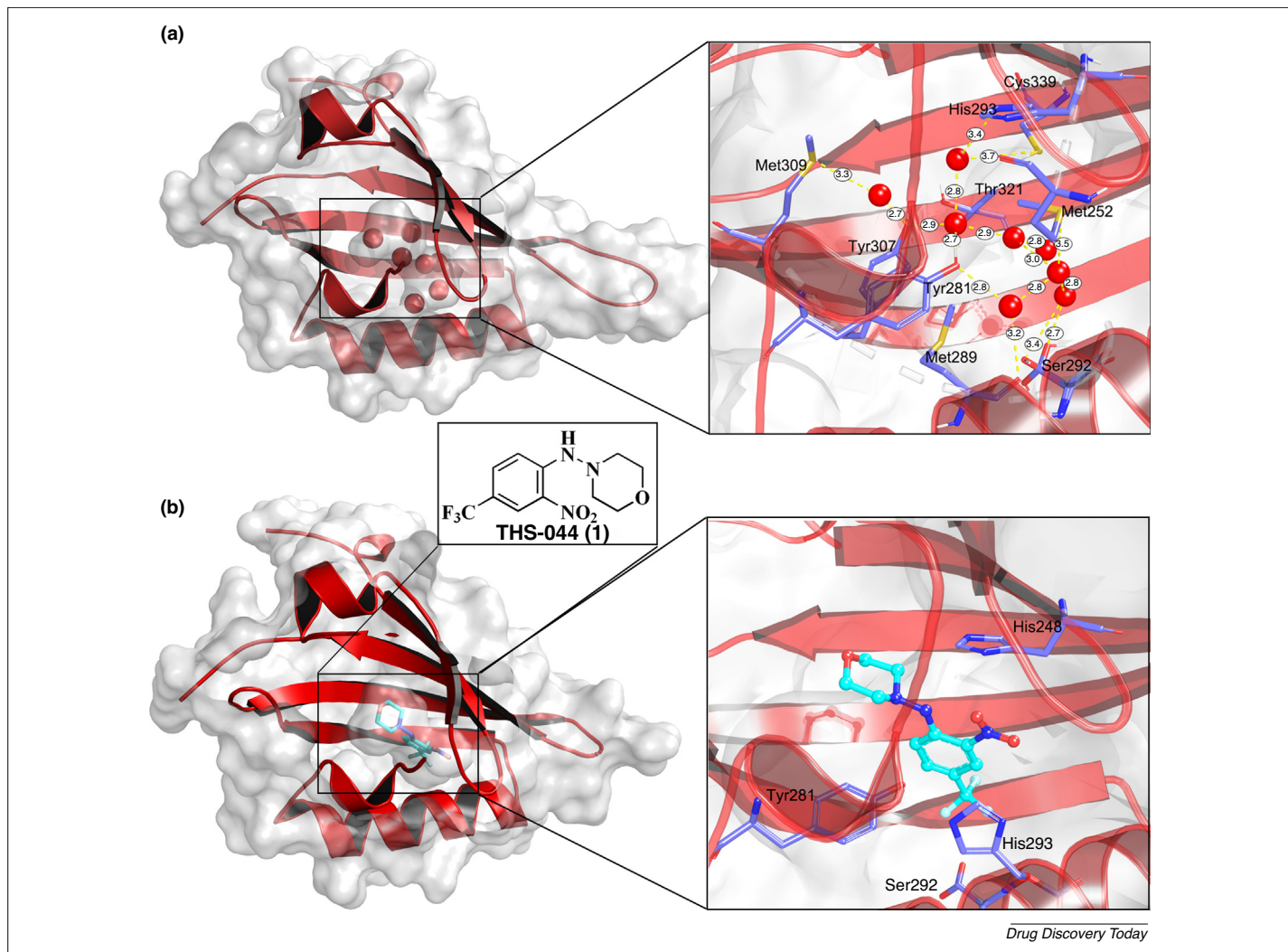


FIGURE 2

Discovery of the internal cavity of HIF-2 α . (a) The 290 Å³ cavity (grey surface) inside hypoxia-inducible factor 2 (HIF-2)- α and the eight ordered, bound water molecules (red spheres) forming a hydrogen bond network with the polar residues around the cavity. The distances between individual atoms are marked as black numbers (in Angstroms) in white boxes. [Protein data bank (PDB) ID: 3F1P]. (b) **THS-044** (cyan stick) occupies the cavity (PDB ID: 3F1O).

[43]. In 2019, Wu *et al.* reported a HIF-2 α allosteric inhibition mechanism in detail [44]. The complex structure (PDB ID: 6E3S) comprising **PT2385** (**2**), a HIF-2 α inhibitor in a clinical Phase II trial, and the HIF-2 α -ARNT heterodimer, was obtained at 3 Å resolution. The superposition of this crystal structure and apo HIF-2 α -ARNT (PDB ID: 4ZP4) indicated that **PT2385** caused a dramatic conformational change of the His293 and Met252 residues in the HIF-2 α -PASB domain (Fig. 3a): the imidazole ring of His293 underwent a 75° rotation so that the nitrogen atom on the imidazole ring could form a hydrogen bond with the hydroxyl group of **PT2385**. Furthermore, **PT2385** occupied the position of the apo Met252 side chain and squeezed the side chain towards the binding surface of HIF-2 α -PASB and ARNT-PASB. This change resulted in varying degrees of shifting of the residue positions on the binding surface, weakening the binding capacity between the two PASB domains [44] (Fig. 3a).

In addition to the characterization by crystallography, mutation strategies have also been used to explain the mechanism of HIF-2 α inhibition. The amino acids at the junction of the two PASB domains were mutated, and then co-immunoprecipitation (co-IP) assays were performed to verify whether the mutation affected dimerization [11]. The results of the mutagenesis tests indicated that most of the mutations significantly impaired the dimerization of the two proteins. This conclusion further demonstrates that altering the Met252 conformation is key to allosteric inhibition of HIF-2 activity.

To explore commonalities of different types of HIF-2 α inhibitor, four crystal structures containing different inhibitors (**THS-044**, **PT2385**, **3** and **4**) were superimposed with apo HIF-2 α -PASB using the 'superimpose proteins' tool of the Discovery Studio Client 4.0 (Fig. 4b). The results showed that, compared with the apo protein, the conformation of His293 and Met252 was significantly changed in all four superimposition structures (Fig. 3b). **THS-044** and

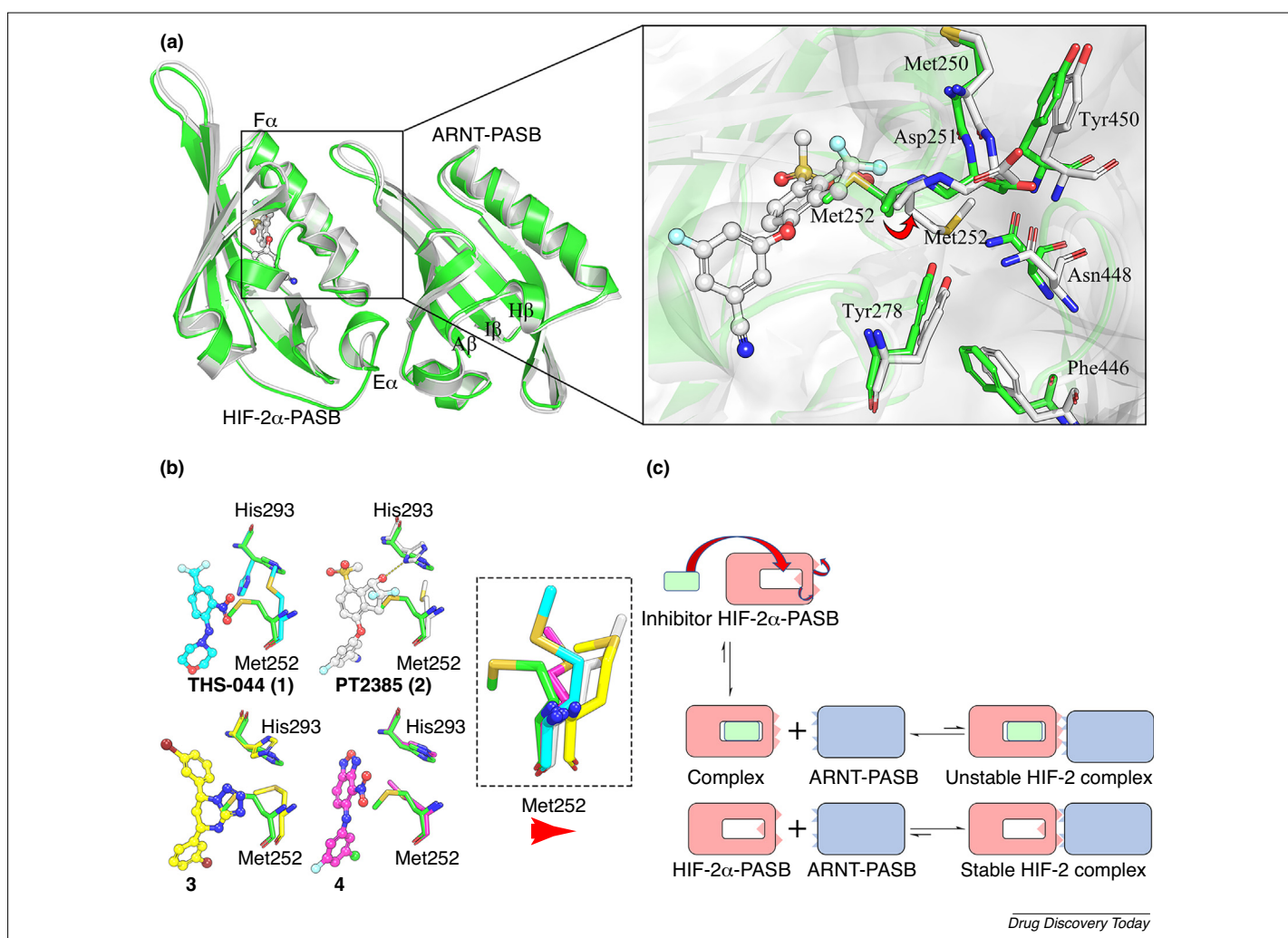


FIGURE 3

Allosteric mechanism of HIF-2 α inhibitors. (a) Overlay of crystal structure of **PT2385** and hypoxia-inducible factor 2 (HIF-2) complex [Protein data bank (PDB) ID: 6E3S, white] and apo HIF-2 complex (PDB ID: 4ZP4, green). The HIF-2 α -PASB and aryl hydrocarbon receptor nuclear translocator (ARNT)-PASB domains are linked by their E α , F α , A β , I β , and H β structures, respectively. The addition of **PT2385** moves the Met252 (white stick) side chain in the HIF-2 α -PASB domain to the junction (white stick), impairing the binding affinity of the two proteins. (b) Under the action of four inhibitors, the conformation of His293 and Met252 residues in the HIF-2 α -PASB domain changed to varying degrees. His293 and Met252 in the apo HIF-2 α -PASB domain are shown as green sticks (PDB ID: 3F1P). The crystal structure containing **THS-044** is shown as a light-blue stick (PDB ID: 3F1O), compound **3** is shown as a yellow stick (PDB ID: 4XT2), compound **4** as a magenta stick (PDB ID: 4GHI), and **PT2385** as a white stick (PDB ID: 5TBM). Of these, **PT2385** affected the greatest Met252 side chain conformation change. (c) Schematic diagram of the allosteric inhibitory mechanism.

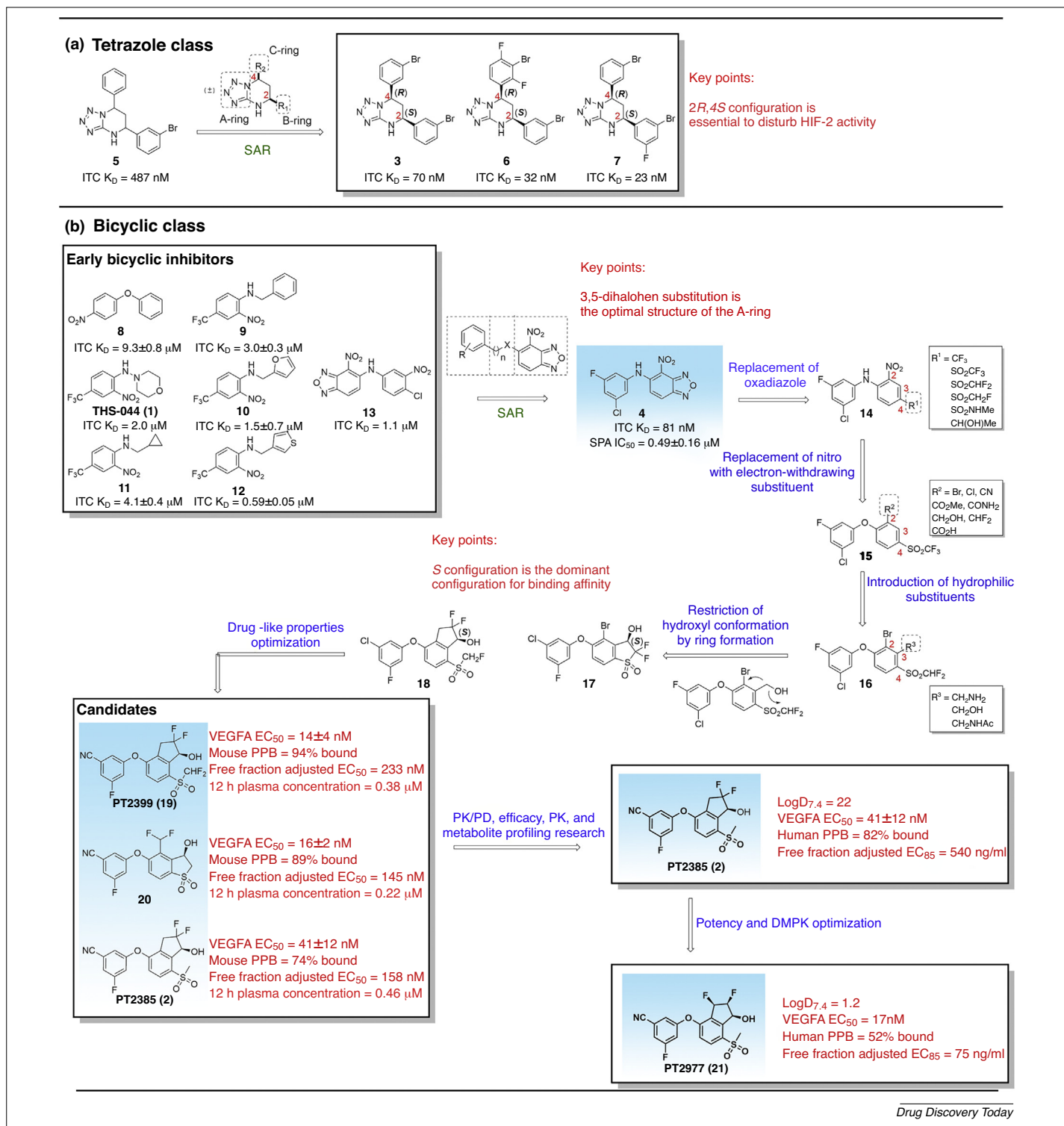


FIGURE 4

Schematic diagram of hypoxia-inducible factor 2 (HIF-2) inhibitor optimization. (a) The tetrazole class HIF-2 α inhibitor. (b) Development of the bicyclic class HIF-2 α inhibitors. Initially, a series of bicyclic compounds (such as compounds 1 and 8–12) that inhibit HIF-2 activity were obtained by high-throughput screening. Subsequent to the preliminary structure–activity relationship (SAR) study of compound 13, compound 4 exhibited the highest binding affinity. Following this, compound 4 was used as the starting point for further in-depth four-step structure-based modification and druggability optimization to obtain PT2385, which was first selected for clinical trials. After further optimization of the drug metabolism and pharmacokinetics (DMPK) profile of PT2385, PT2977 was obtained as a second-generation HIF-2 α inhibitor.

PT2385 utilized the rotatability of the His293 side chain to form hydrogen bonds, enhancing their binding to the cavity; this confirmed that hydrogen bond formation with His293 should be an important consideration in the design of an inhibitor. In the four structures, movement of the side chain of Met252 was significant, and the results appeared to indicate a certain degree of positive correlation between the angle of Met252 flipping and the inhibitory ability of the compounds (Fig. 3b).

From these structural principles, it is known that HIF-2 α inhibitors require two abilities: first, the ability to bind to the internal cavity of PASB, and second, the ability to change the conformation of Met252 [45]. Therefore, the binding constant K_D is not the only criterion for evaluating the ability of a compound to inhibit HIF-2 α ; whether it can trigger a biological effect caused by the decrease of HIF-2 activity is also an important index for evaluating HIF-2 α inhibitors, which can be tested via assays such as luciferase reporter gene assay and VEGFA ELISA assay.

Structural optimization of HIF-2 α inhibitors

Currently, HIF-2 α inhibitors that bind to the HIF-2 α -PASB domain can be roughly divided into two classes of bicyclic and tetrazole scaffolds. The first tetrazole HIF-2 α inhibitor **5** was obtained during high-throughput screening (HTS) [46]. In 2015, Tambar *et al.* synthesized a series of tetrazole compounds with different B and C ring substitutions of 5-aminotetrazole and substituted chalcone [47]. Interestingly, only compounds in the 2*S*,4*R* configuration had an inhibitory effect on HIF-2 α , whereas compounds in the 2*R*,4*S* configuration had little activity. Ultimately, **6** and **7** with the best binding affinity were obtained (Fig. 4a). Furthermore, compound **7** was able to effectively inhibit the mRNA level of the HIF-2 α target gene *EPO* in Hep3B cells under hypoxic conditions (1% O₂ concentration) [47]. However, such compounds might be impractical because of insufficient hydrophilicity. No follow-up studies have been reported as yet.

Present research on HIF-2 α inhibitors mainly focuses on bicyclic compounds, most of which have two aromatic rings connected by one or two atoms. In 2009, Gardner *et al.* screened 200 000 structurally diverse small molecules by NMR-based ligand binding assay [8]. Several compounds exhibited low micromolar equilibrium dissociation constants (compounds **1** and **8–13**) [8], of which oxadiazole **13** had the best protein binding affinity and was chosen as the starting point for SAR research [42]. The structure of **13** was divided into three parts: the A-ring, B-ring, and the connecting atom (Fig. 4b). It was concluded that the nitro-oxadiazole structure in ring A is important for activity: the removal or substitution of the oxadiazole structure by benzimidazole resulted in a substantially decreased binding affinity. Similarly, removal of the nitro group or its reduction to the amine also decreased in activity. The activity was optimal when the connecting atom was a nitrogen atom. The best cavity-matching and binding affinity was obtained when the A-ring was *meta*-dihalo-substituted. As a result of structural optimization, compound **4** was obtained with the highest protein binding affinity of $K_D = 81$ nM (Fig. 4b). Subsequently, real-time fluorescence quantitative PCR (RT-PCR) and co-IP assays were conducted to verify that compound **4** can selectively inhibit HIF-2 α -related downstream genes expression *in vitro* without affecting HIF-1 α [48].

Although compound **4** has good binding affinity with HIF-2 α , its ability to inhibit HIF-2 α *in vivo* is not as expected, which might

be because of its inconspicuous interference with Met252 conformation in the HIF-2 α -PASB domain (Fig. 3b, magenta stick). A new round of structural optimization starting with **4** was conducted by Peloton Therapeutics, Inc. [45] (Fig. 4b). The scintillation proximity assay (SPA) was used to detect dissociation of the protein–compound interaction, and HIF-2 α -driven HRE-dependent luciferase and VEGFA ELISA assays were carried out to evaluate HIF-2 α inhibition. At the beginning of optimization, it was believed that the interaction between Tyr281 and electron-deficient B-ring was key. Some strong electron-withdrawing groups were introduced to replace the B-ring oxadiazole (**14**) and nitro (**15**) (Fig. 4b). The activity results indicated that the stronger the electron-withdrawing ability of the introduced group, the lower the electron density of the A-ring, and the better the activity. Furthermore, when large hydrophilic substituents were incorporated at position 3 of the B-ring (**16**), an unexpected significant increase in activity was achieved when methylol was substituted, which formed a hydrogen-bond network with His293, Tyr281, and a water molecule. To enhance this interaction mode, two types of cyclic scaffold were designed to constrain this hydroxyl to form stronger hydrogen bonds (**17** and **18**). The activity data indicated higher protein affinity of (*S*)-**17** and (*S*)-**18** than their corresponding enantiomers, and that the hydroxyl group of the *S* configuration was an essential group for binding. Compounds **PT2399** (**19**), **20**, and **PT2385** (**2**) were chosen as candidates. After a series of studies on pharmacokinetics/pharmacodynamics (PK/PD), efficacy, PK and metabolic profiling, compound **2** (**PT2385**) with the best balance of activity and druggability (VEGFA EC₅₀ = 41 ± 12 nM, free fraction adjusted EC₅₀ = 158 nM) was selected as the first HIF-2 α inhibitor to enter clinical trials [44,45] (Fig. 4b).

In a clinical Phase I trial, **PT2385** showed a favorable safety profile and was potent in patients with advanced ccRCC [49]. However, in clinical PK studies, **PT2385** revealed disadvantageous interindividual PK variability (free fraction adjusted to EC₈₅ = 540 ng/ml). Based on the analysis of clinical PK data, excessive glucuronidation of its hydroxyl group was considered to be the reason for the unfavorable PK properties of **PT2385** [50]. To decrease the glucuronidation of **PT2385** and improve bioavailability, Peloton Therapeutics developed the second-generation HIF-2 α inhibitor **PT2977** (**21**) (Fig. 4b). Structurally, **PT2977** removes a fluorine atom adjacent to the hydroxyl group, increasing the p*K*_a of the hydroxyl group and thereby weakening the glucuronidation reactivity (free fraction adjusted EC₈₅ = 75 ng/ml). The introduction of a fluorine atom in the B-ring benzyl group weakens the B-ring electron cloud density to enhance the interaction of the B-ring and Tyr281 to improve potency (VEGFA EC₅₀ = 17 nM). In preclinical xenograft models of ccRCC, **PT2977** was approximately tenfold more potent than **PT2385**. Clinical trials of **PT2977** revealed its good safety profile and promising efficacy with a confirmed response rate of 22%. According to reports by Peloton Therapeutics, Inc., a **PT2977** monotherapy Phase III trial in patients with previously treated advanced RCC is planned [50] (Fig. 4b).

Concluding remarks

Inactivation of *VHL* occurs in >90% of ccRCCs, which leads to an increase in the expression level of HIF-2 α . Overexpression of HIF-2 α leads to transcriptional activation of its downstream genes.

These gene expression products are involved in angiogenesis, invasion and metastasis, cell cycle, and metabolism disruption in the progression of ccRCC. Direct inhibition of HIF-2 α might be a more effective strategy than inhibition of angiogenic pathways alone to treat *VHL*-deficient ccRCC. HIF-2 α allosteric inhibitors interfere with the dimerization of the two subunits HIF-2 α and ARNT by altering the Met252 conformation inside the cavity of the HIF-2 α -PASB domain, thereby inhibiting HIF-2 activity. The representative HIF-2 α inhibitor **PT2977** has an excellent PK profile and encouraging clinical activity in clinical Phase II trials for the treatment of advanced RCC.

Although HIF-2 α inhibitors **PT2385** and **PT2977** have exhibited favorable performance in the treatment of ccRCC, the problem of drug resistance because of tumor mutations also exists. A preclinical study in **PT2399** (an analog of **PT2385**, Fig. 4b) reported that ccRCC xenografts in mice acquired resistance after long-term use of **PT2399**. The two leading mutations were to G323E of HIF-2 α and F446 L of ARNT [51,52]. In a recent study, Wu *et al.* used a TR-FRET-based assay to analyze the effects of two mutations on **PT2385** activity. The HIF-2 α G323E mutation had little effect on the binding affinity of the dimer itself, but the inhibiting effect of **PT2385** was almost lost; they speculated that this mutation restricted entry of **PT2385** into the cavity. The other mutation to F446 L of ARNT enhanced the binding affinity of the two subunits, and **PT2385** was able to inhibit subunit dimerization in a dose-dependent manner but with strikingly reduced activity [44]. Therefore, areas of future research focus could include the discovery of HIF-2 α inhibitors that can overcome drug-resistant mutations, as well as the possible design in

light of previous reports of novel HIF-2 α inhibitors for other drug binding pockets of HIF-2 α (such as the PAS-A domain). In addition to the direct allosteric regulation of HIF by small molecules, there are also many indirect regulatory strategies. It is also possible for a compound to have a good effect on patients with ccRCC through such indirect regulatory strategies [53].

Wu *et al.* first reported HIF-2 agonists **M1001** and **M1002** in 2019, which bind to the same pocket as HIF-2 inhibitors [44]. After binding to the pocket, Tyr281 is squeezed from the inside of the cavity to the subunit binding surface to form hydrogen bonds with the Tyr456 of ARNT. This change enhances the stability of the HIF-2 complex and increases its activity. The discovery of HIF-2 agonists offers new possibilities for the treatment of some HIF-2 α -deficient diseases, such as renal anemia. Studies demonstrated that **M1002** has little effect on HIF-2 α target genes, but can significantly elevate intracellular EPO levels when used in combination with a PHD inhibitor, which can upregulate the content of HIF-2 α [44]. Thus, designing or screening more effective HIF-2 agonists might be a new strategy for the treatment of renal anemia.

Acknowledgments

This work was supported by grants from the National Natural Science Foundation of China (Grants 81973173 and 81773571), Jiangsu Province Funds for Excellent Young Scientists (Grant BK20170088), the Fundamental Research Funds for the Central Universities (Grants 2632017ZD03 and 2632019ZD14), and the Jiangsu Qing Lan Project and 333 Project. All figures showing binding modes were generated using PyMol (www.pymol.org).

References

- Bray, F. *et al.* (2018) Global cancer statistics 2018: GLOBOCAN estimates of incidence and mortality worldwide for 36 cancers in 185 countries. *CA Cancer J. Clin.* 68, 394–424
- Hsieh, J.J. *et al.* (2017) Renal cell carcinoma. *Nat. Rev. Dis. Primers* 3, 17009
- Gossage, L. *et al.* (2014) VHL, the story of a tumour suppressor gene. *Nat. Rev. Cancer* 15, 55–64
- Rathmell, W.K. and Chen, S. (2008) VHL inactivation in renal cell carcinoma: implications for diagnosis, prognosis and treatment. *Expert Rev. Anticancer Ther.* 8, 63–73
- Melendez-Rodriguez, F. *et al.* (2018) Hypoxia-inducible factor 2-dependent pathways driving von Hippel-Lindau-deficient renal cancer. *Front. Oncol.* 8, 214
- Murakami, A. *et al.* (2017) Context-dependent role for chromatin remodeling component PBRM1/BAF180 in clear cell renal cell carcinoma. *Oncogenesis* 6, 1–10
- Biswas, S. *et al.* (2010) Effects of HIF-1 α and HIF2 α on growth and metabolism of clear-cell renal cell carcinoma 786-0 xenografts. *J. Oncol.* 2010, 1–14
- Scheuermann, T.H. *et al.* (2009) Artificial ligand binding within the HIF2 PAS-B domain of the HIF2 transcription factor. *Proc. Natl. Acad. Sci. U. S. A.* 106, 450–455
- Key, J. *et al.* (2009) Principles of ligand binding within a completely buried cavity in HIF2 α PAS-B. *J. Am. Chem. Soc.* 131, 17647–17654
- Jonasch, E. *et al.* (2019) An open-label phase II study to evaluate PT2977 for the treatment of von Hippel-Lindau disease-associated renal cell carcinoma. *J. Clin. Oncol.* 37, TPS680
- Wu, D. *et al.* (2015) Structural integration in hypoxia-inducible factors. *Nature* 524, 303–308
- Tarhonskaya, H. *et al.* (2015) Kinetic investigations of the role of factor inhibiting hypoxia-inducible factor (FIH) as an oxygen sensor. *J. Biol. Chem.* 290, 19726–19742
- Yan, Q. *et al.* (2007) The hypoxia-inducible factor 2 α N-terminal and C-terminal transactivation domains cooperate to promote renal tumorigenesis *in vivo*. *Mol. Cell Biol.* 27, 2092–2102
- Schito, L. and Semenza, G.L. (2016) Hypoxia-inducible factors: master regulators of cancer progression. *Trends Cancer* 2, 758–770
- Simon, T. *et al.* (2017) Direct effects of anti-angiogenic therapies on tumor cells: VEGF signaling. *Trends Mol. Med.* 23, 282–292
- Elvert, G. *et al.* (2003) Cooperative interaction of hypoxia-inducible factor-2 α (HIF-2 α) and Ets-1 in the transcriptional activation of vascular endothelial growth factor receptor-2 (Flk-1). *J. Biol. Chem.* 278, 7520–7530
- Eilken, H.M. and Adams, R.H. (2010) Dynamics of endothelial cell behavior in sprouting angiogenesis. *Curr. Opin. Cell Biol.* 22, 617–625
- Nilsson, I. *et al.* (2004) Differential activation of vascular genes by hypoxia in primary endothelial cells. *Exp. Cell Res.* 299, 476–485
- Loeffler, S. *et al.* (2005) Interleukin-6 induces transcriptional activation of vascular endothelial growth factor (VEGF) in astrocytes *in vivo* and regulates VEGF promoter activity in glioblastoma cells via direct interaction between STAT3 and Sp1. *Int. J. Cancer* 115, 202–213
- Oehler, M.K. *et al.* (2002) Adrenomedullin promotes formation of xenografted endometrial tumors by stimulation of autocrine growth and angiogenesis. *Oncogene* 21, 2815–2821
- Ricketts, C.J. and Linehan, W.M. (2017) Insights into epigenetic remodeling in VHL-deficient clear cell renal cell carcinoma. *Cancer Discov.* 7, 1221–1223
- Zhao, D. *et al.* (2014) Upregulation of HIF-2 α induced by sorafenib contributes to the resistance by activating the TGF- α /EGFR pathway in hepatocellular carcinoma cells. *Cell. Signal.* 26, 1030–1039
- Bertout, J.A. *et al.* (2009) HIF2 α inhibition promotes p53 pathway activity, tumor cell death, and radiation responses. *Proc. Natl. Acad. Sci. U. S. A.* 106, 14391–14396
- Gordan, J.D. *et al.* (2007) HIF and c-Myc: sibling rivals for control of cancer cell metabolism and proliferation. *Cancer Cell* 12, 108–113
- Gramp, S. *et al.* (2016) Genetic variation at the 8q24.21 renal cancer susceptibility locus affects HIF binding to a MYC enhancer. *Nat. Commun.* 7, 13183
- Schodel, J. *et al.* (2012) Common genetic variants at the 11q13.3 renal cancer susceptibility locus influence binding of HIF to an enhancer of cyclin D1 expression. *Nat. Genet* 44, 420–425
- Elorza, A. *et al.* (2012) HIF2 α acts as an mTORC1 activator through the amino acid carrier SLC7A5. *Mol. Cell* 48, 681–691

- 28 Betsunoh, H. *et al.* (2013) Increased expression of system large amino acid transporter (LAT)-1 mRNA is associated with invasive potential and unfavorable prognosis of human clear cell renal cell carcinoma. *BMC Cancer* 13, 509
- 29 Onishi, Y. *et al.* (2019) Hypoxia affects SLC7A5 expression through HIF-2 α in differentiated neuronal cells. *FEBS Open Biol.* 9, 241–247
- 30 Micucci, C. *et al.* (2015) HIF2 α is involved in the expansion of CXCR4-positive cancer stem-like cells in renal cell carcinoma. *Br. J. Cancer* 113, 1178–1185
- 31 Rasti, A. *et al.* (2017) Reduced expression of CXCR4, a novel renal cancer stem cell marker, is associated with high-grade renal cell carcinoma. *J. Cancer Res. Clin. Oncol.* 143, 95–104
- 32 Rankin, E.B. *et al.* (2014) Direct regulation of GAS6/AXL signaling by HIF promotes renal metastasis through SRC and MET. *Proc. Natl. Acad. Sci. U. S. A.* 111, 13373–13378
- 33 Bourboulia, D. and Stetler-Stevenson, W.G. (2010) Matrix metalloproteinases (MMPs) and tissue inhibitors of metalloproteinases (TIMPs): Positive and negative regulators in tumor cell adhesion. *Semin. Cancer Biol.* 20, 161–168
- 34 Chen, Y.S. *et al.* (2016) Dicer suppresses MMP-2-mediated invasion and VEGFA-induced angiogenesis and serves as a promising prognostic biomarker in human clear cell renal cell carcinoma. *Oncotarget* 7, 84299–84313
- 35 Koh, M.Y. *et al.* (2011) The hypoxia-associated factor switches cells from HIF-1 α to HIF-2 α -dependent signaling promoting stem cell characteristics, aggressive tumor growth and invasion. *Cancer Res.* 71, 4015–4027
- 36 Petrella, B.L. *et al.* (2005) Identification of membrane type-1 matrix metalloproteinase as a target of hypoxia-inducible factor-2 α in von Hippel-Lindau renal cell carcinoma. *Oncogene* 24, 1043–1052
- 37 Emerling, B.M. *et al.* (2013) Identification of CDCP1 as a hypoxia-inducible factor 2 α (HIF-2 α) target gene that is associated with survival in clear cell renal cell carcinoma patients. *Proc. Natl. Acad. Sci. U. S. A.* 110, 3483–3488
- 38 Salama, M.F. *et al.* (2015) A novel role of sphingosine kinase-1 in the invasion and angiogenesis of VHL mutant clear cell renal cell carcinoma. *FASEB J.* 29, 2803–2813
- 39 Chan, D.A. *et al.* (2011) Targeting GLUT1 and the Warburg effect in renal cell carcinoma by chemical synthetic lethality. *Sci. Transl. Med.* 3, 94ra70
- 40 Zhang, T. *et al.* (2013) The contributions of HIF-target genes to tumor growth in RCC. *PLoS One* 8, e80544
- 41 Qiu, B. *et al.* (2015) HIF2 α -dependent lipid storage promotes endoplasmic reticulum homeostasis in clear-cell renal cell carcinoma. *Cancer Discov.* 5, 652–667
- 42 Rogers, J.L. *et al.* (2013) Development of inhibitors of the PAS-B domain of the HIF-2 α transcription factor. *J. Med. Chem.* 56, 1739–1747
- 43 Wallace, E.M. *et al.* (2016) A small-molecule antagonist of HIF2 α is efficacious in preclinical models of renal cell carcinoma. *Cancer Res.* 76, 5491–5500
- 44 Wu, D. *et al.* (2019) Bidirectional modulation of HIF-2 activity through chemical ligands. *Nat. Chem. Biol.* 15, 367–376
- 45 Wehn, P.M. *et al.* (2018) Design and activity of specific hypoxia-inducible factor-2 α (HIF-2 α) inhibitors for the treatment of clear cell renal cell carcinoma: discovery of clinical candidate (S)-3-((2,2-difluoro-1-hydroxy-7-(methylsulfonyl)-2,3-dihydro-1H-inden-4-yl)oxy)-5-fluorobenzonitrile (PT2385). *J. Med. Chem.* 61, 9691–9721
- 46 Dougherty, A.M. *et al.* (2007) A substituted tetrahydro-tetrazolo-pyrimidine is a specific and novel inhibitor of hepatitis B virus surface antigen secretion. *Antimicrob. Agents Ch.* 51, 4427–4437
- 47 Scheuermann, T.H. *et al.* (2015) Isoform-selective and stereoselective inhibition of hypoxia inducible factor-2. *J. Med. Chem.* 58, 5930–5941
- 48 Scheuermann, T.H. *et al.* (2013) Allosteric inhibition of hypoxia inducible factor-2 with small molecules. *Nat. Chem. Biol.* 9, 271–276
- 49 Courtney, K.D. *et al.* (2017) Phase I dose-escalation trial of PT2385, a first-in-Class hypoxia-inducible factor-2 α antagonist in patients with previously treated advanced clear cell renal cell carcinoma. *J. Clin. Oncol.* 36, 867–874
- 50 Xu, R. *et al.* (2019) 3-[(1S,2S,3R)-2,3-difluoro-1-hydroxy-7-methylsulfonyl-indan-4-yl]oxy-5-fluoro-benzonitrile (PT2977), a hypoxia-inducible factor 2 α (HIF-2 α) inhibitor for the treatment of clear cell renal cell carcinoma. *J. Med. Chem.* 62, 6876–6893
- 51 Chen, W. *et al.* (2016) Targeting renal cell carcinoma with a HIF-2 antagonist. *Nature* 539, 112–117
- 52 Cho, H. *et al.* (2016) On-target efficacy of a HIF-2 α antagonist in preclinical kidney cancer models. *Nature* 539, 107–111
- 53 Li, Z. *et al.* (2019) Small-molecule modulators of the hypoxia-inducible factor pathway: development and therapeutic applications. *J. Med. Chem.* 62, 5725–5749